Supplemental Data

Supplemental Figure 1. Dose dependence and quantitation of synuclein effects on mitochondrial morphology.

(A) Azurite and mitoGFP correlate with the expression of α-synuclein. Hela cells were transfected with cDNAs encoding azurite, mitoGFP and either wild type α-synuclein, A30P α-synuclein, or vector control and immunostained for synuclein. Analysis by linear regression shows that the immunofluorescence for synuclein correlates with azurite and mitoGFP expression. r^2 is the square of the correlation coefficient, and represents the proportion of variability in azurite or mitoGFP fluorescence that is accounted for by the synuclein expreesion level. n=77-148 cells per group

(B) Structural analysis of fragmented mitochondria. HeLa cells were transfected with azurite, mitoGFP and either wild type α-synuclein or vector control. Other HeLa cells were treated with 2 μM cyclosporine (CSA) or 10 μM carbonyl cyanide 3-chlorophenylhydrazone (CCCP) for 50 min (early, E) or 3 hours (late, L). Cells were photographed live and the length, width, length/width, perimeter and area $(\mu M)^2$ of mitochondria quantified using Metamorph software (Universal Imaging). Quantitation confirms that synuclein reduces the length, perimeter, area and axis ratio (length/width), and increases the width of mitochondria ($p<0.001$ versus control by one way ANOVA and Newman-Keuls post hoc test for all parameters). Quantitation of the number of disc-shaped mitochondria per field.

Supplemental Figure 2. α-Synuclein expression is blocked by siRNA.

HeLa cells were transfected with either vector control (con) or synuclein cDNA (syn), in the presence or absence of siRNA to human synuclein (Silencer Select s13204 (1), s13205 (2), s13206 (3)) or control siRNA (Silencer Select negative control 1 (C)). Cell lysates were harvested after 48 hours and immunoblotted for human synuclein and actin (A). siRNA 2 and 3 (but not 1 or C) effectively block synuclein expression. Lysates prepared from HeLa cells transfected with either vector control (con), synuclein (syn), or mutant A30P, A53T or E46K synuclein were immunoblotted for human and total synuclein (B). To compare with endogenous brain levels of synuclein, lysates were also prepared from rat brain.

Supplemental Figure 3. α-Synuclein does not disrupt the morphology of lysosomes or cytoskeleton.

Hela cells stably expressing mitoGFP were transfected with azurite and either vector control (-syn) or wild type α-synuclein (+syn). 48 hours after transfection, the cells were fixed and stained for either the lysosome-associated membrane protein lamp1 (A) or α-tubulin (B). Despite massive mitochondrial fragmentation, the morphology of lysosomes and microtubule cytoskeleton shows no effect of synuclein expression. Scale bars indicate 10 μm.

Supplemental Figure 4. α-Synuclein does not influence peroxisome morphology.

Hela cells were transfected with azurite, mitoGFP and either vector control, α-synuclein, the dominant negative Drp1 mutant K38A, or the combination of α-synuclein and K38A Drp1. 48 hours after transfection, cells were fixed, and immunostained for the peroxisomal membrane protein PMP70 (A). Scale bar indicates 2 μm. Randomized high power fields from individual

cells were then analyzed for mean peroxisome area (B) and the extent of mitochondrial fragmentation (C). α-synuclein fragments mitochondria (C, $p<0.0001$), but does not affect the area or morphology of peroxisomes even after tubulation with K38A (B). Data show mean ± SEM, n=97-134 peroxisomes per group, n=11-12 high power fields of mitochondria per group.

Supplemental Figure 5. Aggregates of mutant huntingtin do not disrupt mitochondrial morphology.

Hela cells were transfected with azurite, mitoGFP and either vector control, wild type α-synuclein, or a fusion of CFP to exon 1 from the huntingtin gene with an expanded trinucleotide repeat (Htt)[56]. 48 hours after transfection, the cells were imaged live (A) and the mitochondrial morphology of randomized cells classified blind to transfection. (B) Htt distribution was categorized as either diffuse or aggregated (inclusion). In contrast to cells expressing α-synuclein that show mitochondrial fragmentation ($p<0.0001$), cells with either diffuse huntingtin or focal aggregates do not differ from control in mitochondrial morphology ($p>0.5$ for both diffuse and aggregated huntingtin versus control). Scale bar indicates 10 μm. n=17-24 cells per group from 2 independent transfections

Supplemental Figure 6. α-Synuclein does not affect mitochondrial membrane potential or superoxide levels.

(A) Hela cells were transfected with either GFP and vector control (-synuclein) or GFP and synuclein (+synuclein). Two days later, cells were incubated for 1 hour with TMRM (1 nM) in the presence or absence of FCCP (5 μM). The cells were then sorted for GFP expression, and TMRM fluorescence stratified on the basis of GFP expression, with untransfected cells in green

and progressively higher GFP expression in dark blue (bottom 0-29% of cells), red (29-59%), light blue (59-90%), purple (90-95%) and yellow (95-100%). Values in the table show mean TMRM fluorescence ± SEM, stratified by GFP expression.

(B) Hela cells were transfected with azurite, mitoGFP and either vector control, α-synuclein or K38A Drp1. Cells were exposed to hydroethidium (3.2 μM), and the relative superoxide levels determined by the initial rate of increase in ethidium fluorescence, as described previously [120]. Despite marked mitochondrial fragmentation, α-synuclein does not increase superoxide levels. In contrast, K38A DRP1 does significantly reduce superoxide ($p<0.01$ by one way ANOVA and Newman-Keuls posthoc test). Values indicate mean ± SEM. n=35-44 cells per condition from more than 2 independent transfections

Supplemental Figure 7. Synuclein does not inhibit mitochondrial fusion.

(A) COS cells were transfected with mitoDsRed and either vector control, α-synuclein, or CFP. The cells were fixed one and two days later, and mitochondrial morphology assessed. α-Synuclein produces mitochondrial fragmentation when compared with control (con) or CFP, at either 24 or 48 hours (n=444-545 cells/group, $p<0.0001$ by chi-square analysis).

(B) COS cells were transfected with vector control (con), α-synuclein (syn) or wild type Drp1 and either mitoGFP or mitoDsRed. 24 hours later, cells expressing mitoGFP or mitoDsRed were plated together and treated with PEG 1500 for 60 s, then cultured for an additional 4, 6.5 or 9 hours before imaging live. Scale bar indicates 10 μm. The mitochondrial fusion of randomized cells was then classified as full, partial or intermediate. All groups undergo fusion over time ($p\leq0.01$), although the rate is somewhat slower in cells expressing either α-synuclein or the

fission protein Drp1 ($p<0.01$ versus control at 4 hours), presumably due to the comparatively small size of mitochondria in these groups. n=18-30 cells per group.

Supplemental Figure 8. Assessment of Neuronal Death Using Automated Microscopy.

An automated microscopy system was used to track single neurons co-expressing mRFP with either synuclein or vector control. Neuronal survival was assessed based on the cell body morphology, visualized with mRFP fluorescence. Loss of mRFP fluorescence indicates loss of membrane integrity and cell death. The morphology of the control neuron (con, upper row) remains intact for at least 122 h. However, in neurons expressing synuclein (middle and lower panels), neurite degeneration (yellow arrows) and rounding of the cell body (white arrows) precede cell death. The survival time of a neuron is determined as the last time point at which the cell body is seen intact. In the middle row, the neuron is last seen alive at 98 h, with the cell body disappearing in the subsequent image. In the lower row, he neuron is last seen alive at 72 h. In subsequent images the cell body is fragmented and then disappears. Scale bar represents 10 μm.

Supplemental Figure 9. Mitochondrial fusion and fission proteins do not block the effect of synuclein.

(A) Hela cells were transfected in the combinations indicated with either vector control (con), α-synuclein (syn), wild type mitofusin (Mfn) 1 or the inactive K88T Mfn1 mutant or wt Mfn2 or its inactive mutant K109A, as well as azurite and mitoGFP. 48 hours after transfection, the live cells were imaged and classified in terms of mitochondrial morphology. The data show the percentage of cells with each morphology. Overexpression of either mitofusin protein fails to

block fragmentation by synuclein. n=22-32 cells/group (B) Hela cells were transfected in the combinations indicated with empty vector control (con), α-synuclein (syn), wild type Drp1, and the dominant negative Drp1 mutant K38A, as well as CFP to identify the transfected cells. 48 hours after transfection, the cells were labeled with MitoTracker 633, imaged, the images randomized and classified in terms of mitochondrial morphology. Scale bar indicates 10 μm. The bar graph indicates the percentage of cells with each morphology. Although K38A Drp1 increases the baseline tubulation of mitochondria, it does not block fragmentation by synuclein. n=19-44 cells per group from 2 independent transfections. Scale bars represent 10 μm.

Supplemental Figure 10. The C-Terminus of α-synuclein is not required for fragmentation.

(A) Hela cells were transfected in the combinations indicated with empty vector control (con), α-synuclein (syn), or C-terminal α-synuclein truncation mutants (syn120, syn110, syn99 and syn80). 48 hours after transfection, cells were selected on the basis of azurite fluorescence, imaged live, the images randomized and mitochondrial morphology classified as described in Fig. 1. Bar graph shows the percentage of cells in each group. All the mutants produce fragmentation ($p<0.001$), but the syn80 construct is less potent than wild type synuclein ($p=0.0016$).

(B) Cells transfected as above were also fixed, immunostained for α-synuclein, and those with a range of synuclein levels classified as in Fig. 1. The number of cells in each group is indicated in parentheses.

Supplemental Figure 11. Clustering of artificial membranes depends on cardiolipin concentration but is independent of protein aggregation.

(A) Artificial liposomes containing PC and decreasing concentrations (50%, 25% and 10%) of cardiolipin (CL) were incubated with or without synuclein for 5 minutes, with a combination of monomeric and trimeric synuclein (20 μM), and the effect on clustering of artificial membranes quantitated. Clustering is observed with liposomes containing 25 or 50% but not 10% CL.

(B) Artificial liposomes containing either CL and PC (1:1) or PC alone were incubated without protein, with a combination of monomeric and trimeric synuclein (0.15 mg/ml, 10 μM) or with aggregated mutant huntingtin (0.34 mg/ml, 10 μM), and the fluorescence of trace NBD conjugated to the N-terminus of 1,2-dioleoyl-sn-glycero-3-phosphocholine (NBD-PC) visualized by light microscopy. "Individual" indicates that essentially all liposomes in a field are isolated, "small clusters" 2-10 liposomes per cluster, and "big clusters" more than 10 liposomes per cluster. In contrast to synuclein, aggregated mutant huntingtin does not produce clustering of CL liposomes.

Supplemental Figure 12. Analysis of recombinant synuclein.

(A) Dynamic light scattering (DLS) of resuspended human α-synuclein shows an average hydrodynamic radius (R_H) of 3.2 nm, consistent with a mixture of partially folded trimer or more compact tetramer. (B) Size exclusion chromatography (SEC) reveals a mixture of roughly 2/3 trimer and 1/3 monomer. (C) Equilibrium analytical ultracentrifugation of synuclein reveals an apparent MW of 34 kD (MWapp), consistent with a mixture of trimer (predicted MW = 42 kD) and monomer (MWmon = 14 kD). (D) DLS of α-synuclein monomers, intermediate oligomers

(oligomer 1) and late oligomers (oligomer 2) after purification by SEC. Monomers have an R_H of 2.8 nm, consistent with a largely unstructured protein of 14 kDa. Oligomer 1 has an average R_H of 4.5 nm, and oligomer 2 of 6.8 nm. (E) SEC of synuclein fractions. The monomer fraction shows a single peak migrating at ~25 kDa, whereas oligomers 1 and 2 contain multiple peaks of ~18 and 55-61 kD. (F) Electron microscopy of late α-synuclein oligomers (left) and fibrils (right). Scale bar indicates 40 nm. (G) Attenuated total reflectance and Fourier transform infrared spectroscopy (ATR-FTIR) secondary structure analysis of the amide I region (1700-1600 cm^{-1}) of α-synuclein monomer and oligomer fractions. Monomers are largely unstructured, whereas oligomer 1 and 2 show progressively more beta-structure at 1630 cm^{-1}.

Supplemental Video 1. Time-lapse movie of Hela cells stably expressing mitoGFP and transiently transfected with α-synuclein and azurite to identify transfected cells.

Cells were incubated overnight at 37º C in 5% CO_2. Images of mitochondria (mitoGFP) were taken every 4 minutes and of the cell body (azurite) every 80 minutes to minimize phototoxicity. Total video length corresponds to 8 hours, played back at 20 minutes real time per second (5 frames/s). Fragmentation develops gradually in transfected cells.

Supplemental Video 2. Time-lapse movie of Hela cells stably expressing mitoGFP and transiently transfected with vector control and azurite, imaged as in Supplemental Video 1.

Total video length corresponds to 5.3 hours, played back at 20 minutes real time per second (5 frames/s). Control cells retain a normal, tubulated mitochondrial morphology throughout the experiment.

Supplemental Video 3. Time-lapse movie of Hela cells stably expressing mitoGFP and transiently transfected (16 hours earlier) with synuclein and azurite.

The cell on the left is transfected with synuclein (based on azurite fluorescence, not shown), whereas the cell on the right presumably expresses little or no synuclein (based on the absence of azurite fluorescence). Total video length corresponds to 39 minutes, played back at 75 seconds real time per second (15 frames/s). Despite the fragmentation, mitochondria in the cell expressing synuclein show robust mitochondrial fusion and fission at multiple sites.

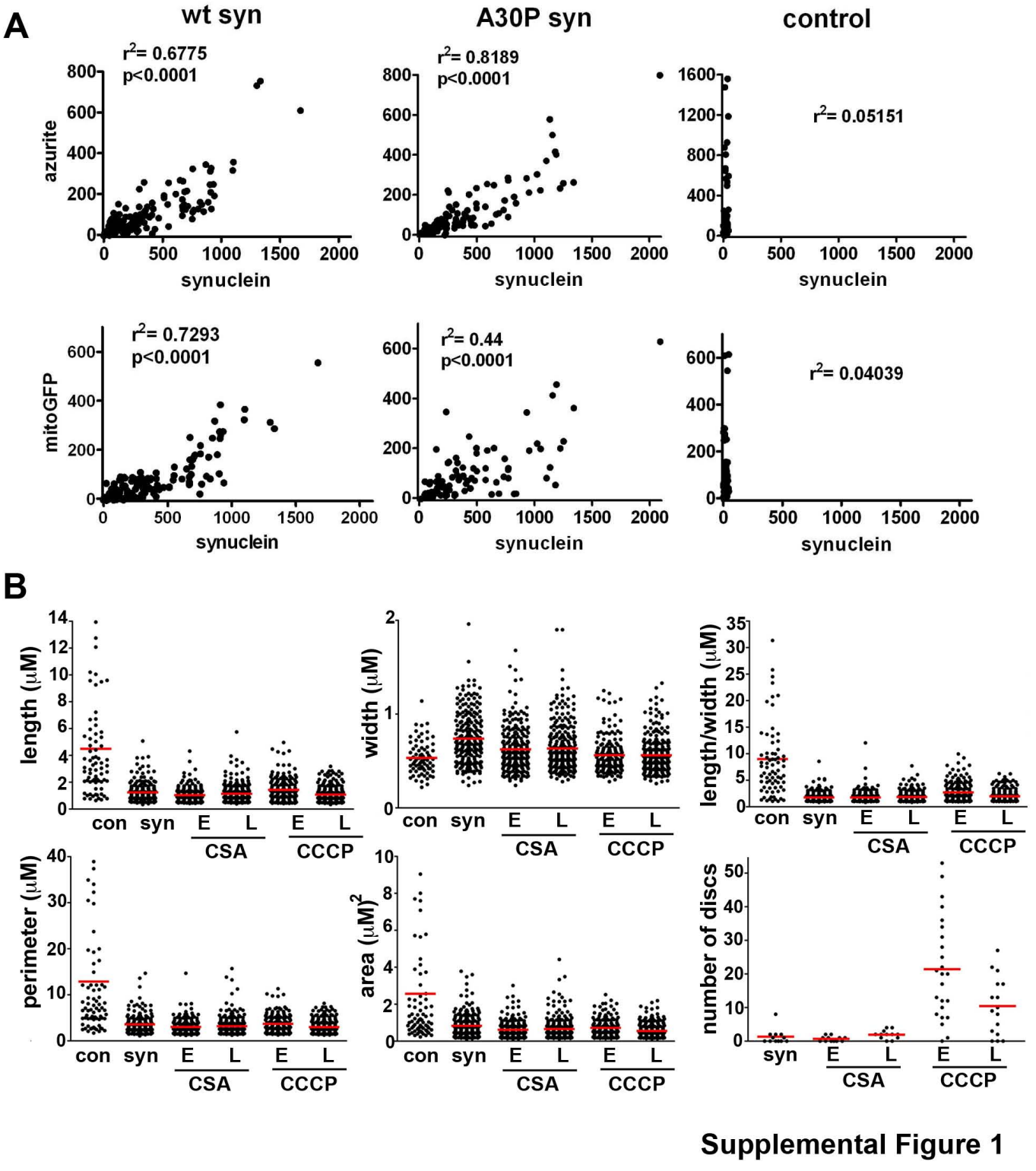

Supplemental Figure 1

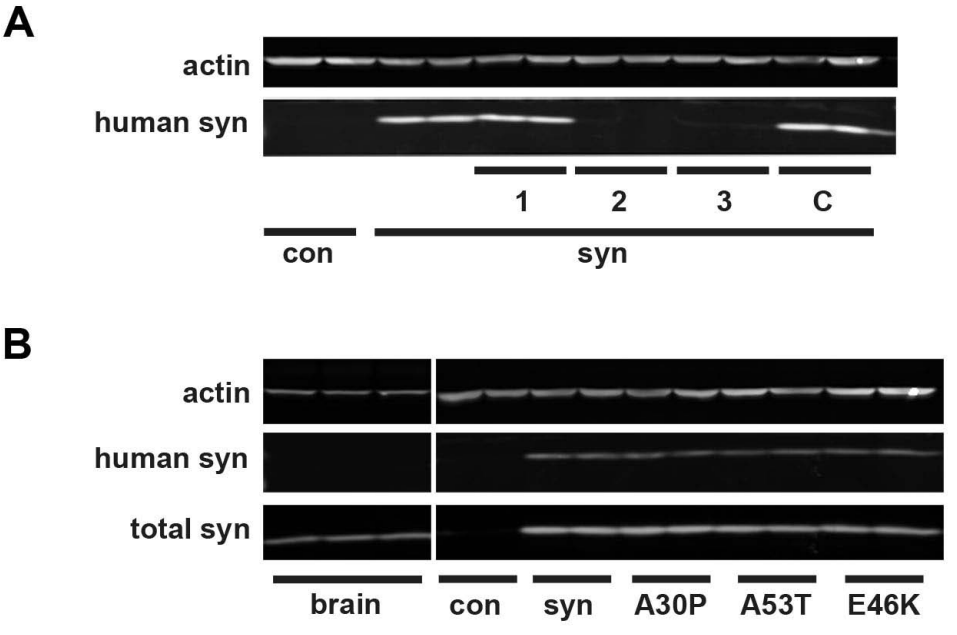

Supplemental Figure 2

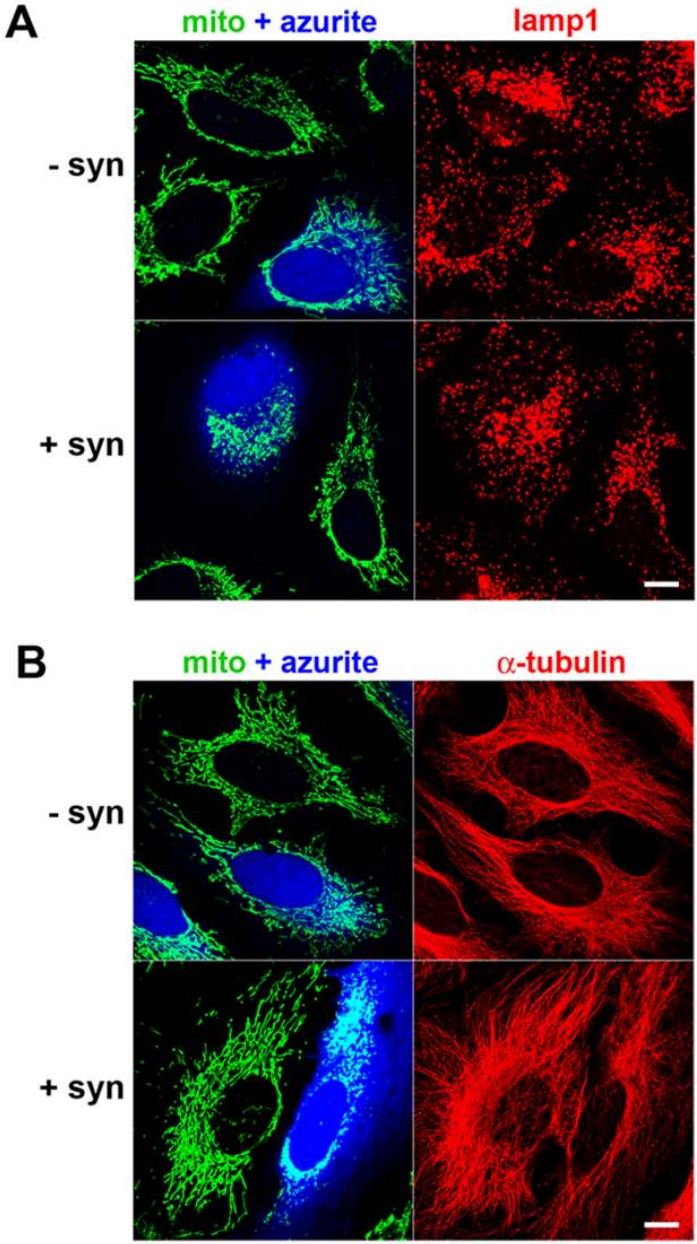

Supplemental Figure 3

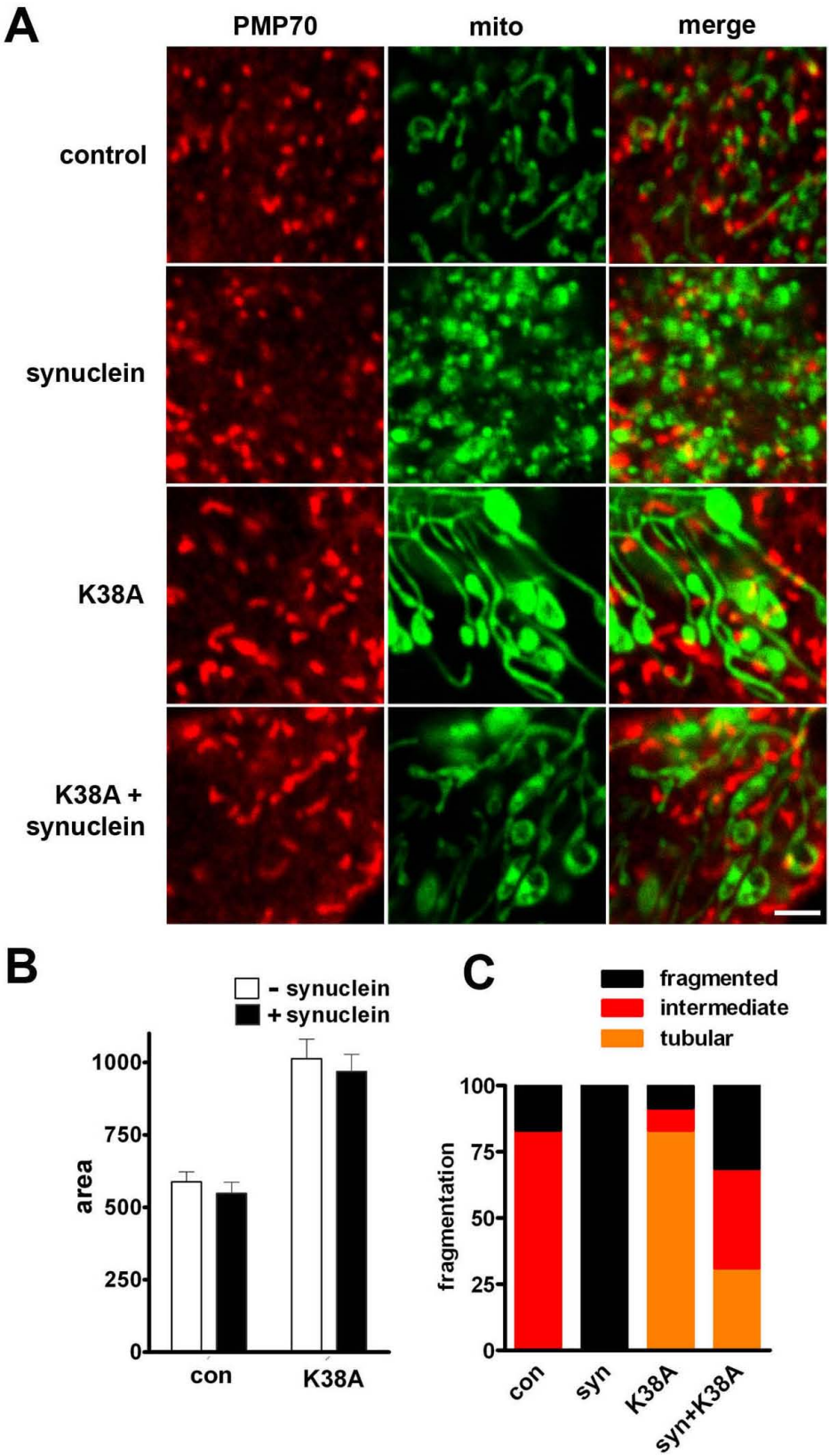

Supplemental Figure 4

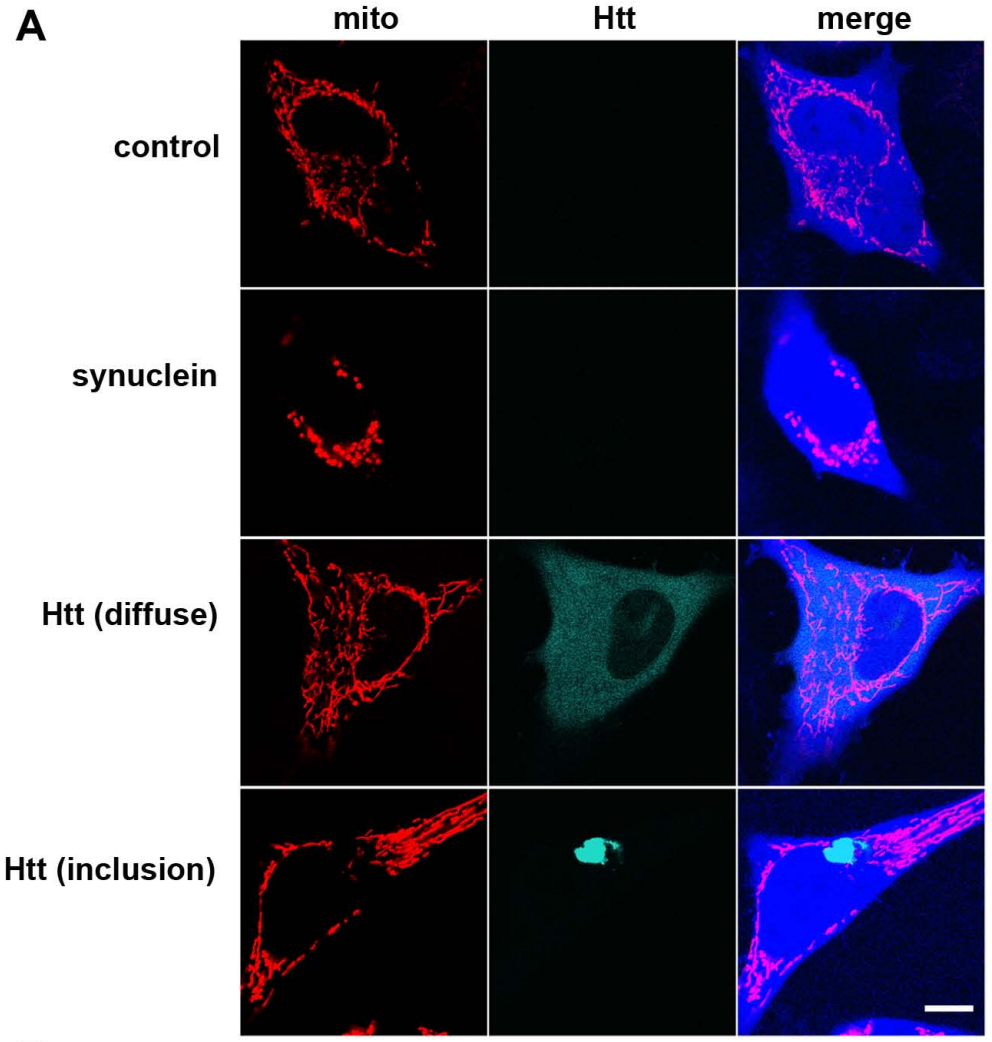

Supplemental Figure 5

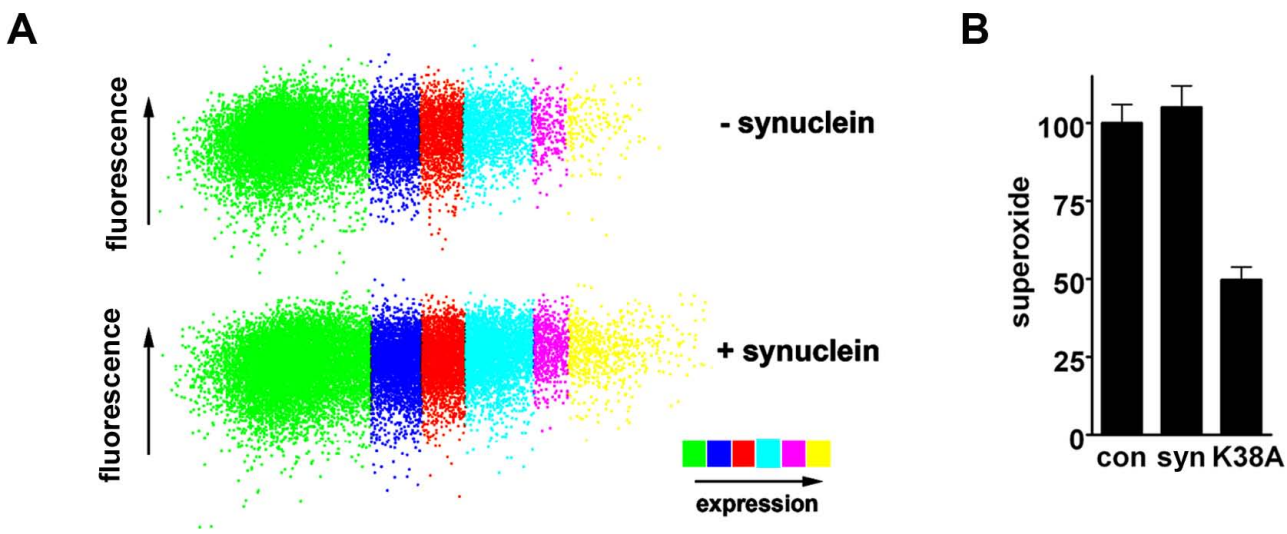

	untransfected	0-29%	29-59%	59-90%	90-95%	95-100%
- syn	5222±130	5488±119	5801±144	6214±143	6511±168	6739±157
- syn +FCCP	1415±44.8	1599±51.9	1608±53.4	1767±61.2	1975±107	2308±67.9
+ syn	6225 ±148	6573±138	6994±140	7538±139	8073±255	8256±180
+ syn -FCCP	1496±69.2	1732±61.0	1742±85.9	1878±73.7	2058±121	2196±71.9

Supplemental Figure 6

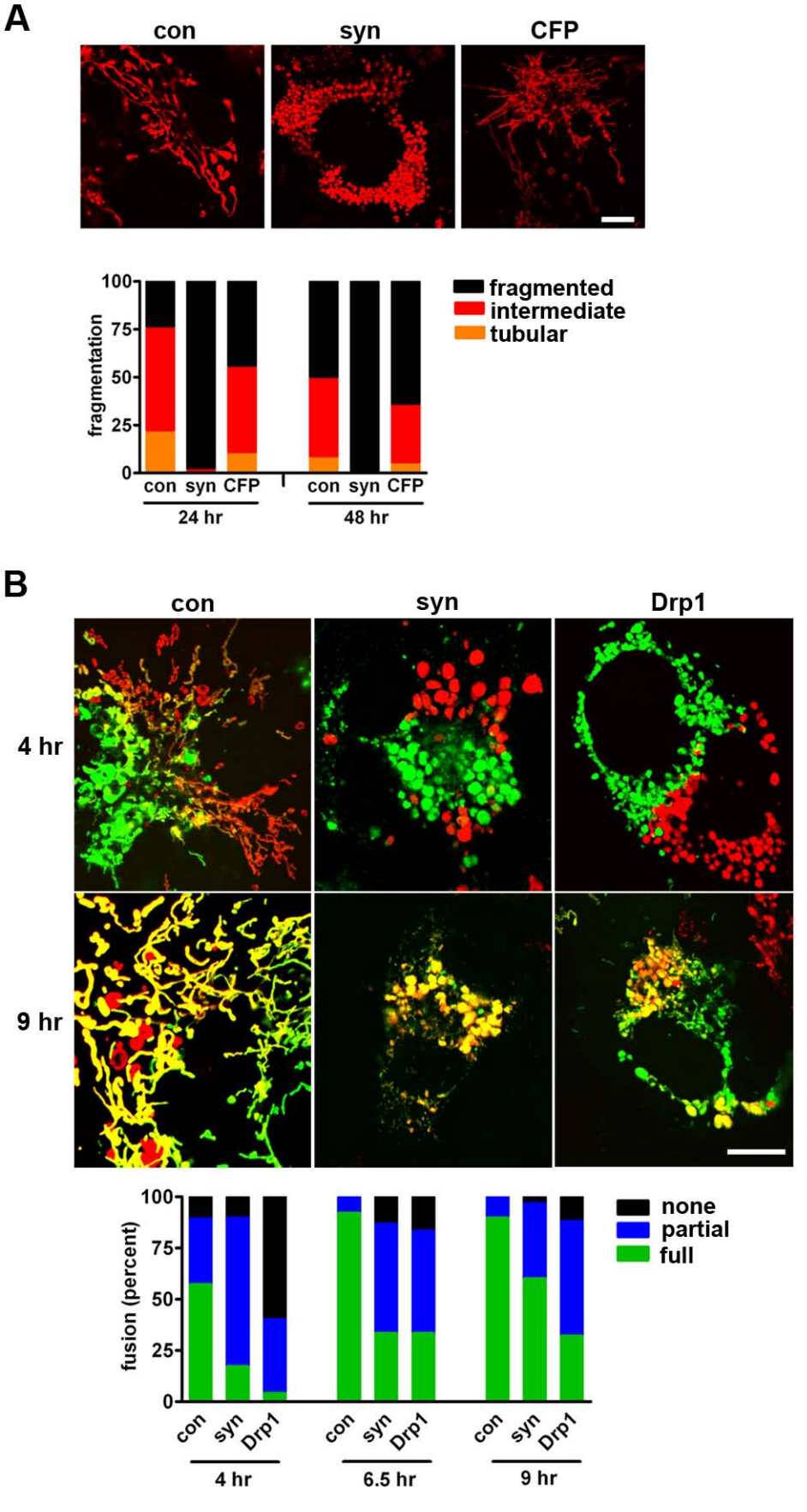

Supplemental Figure 7

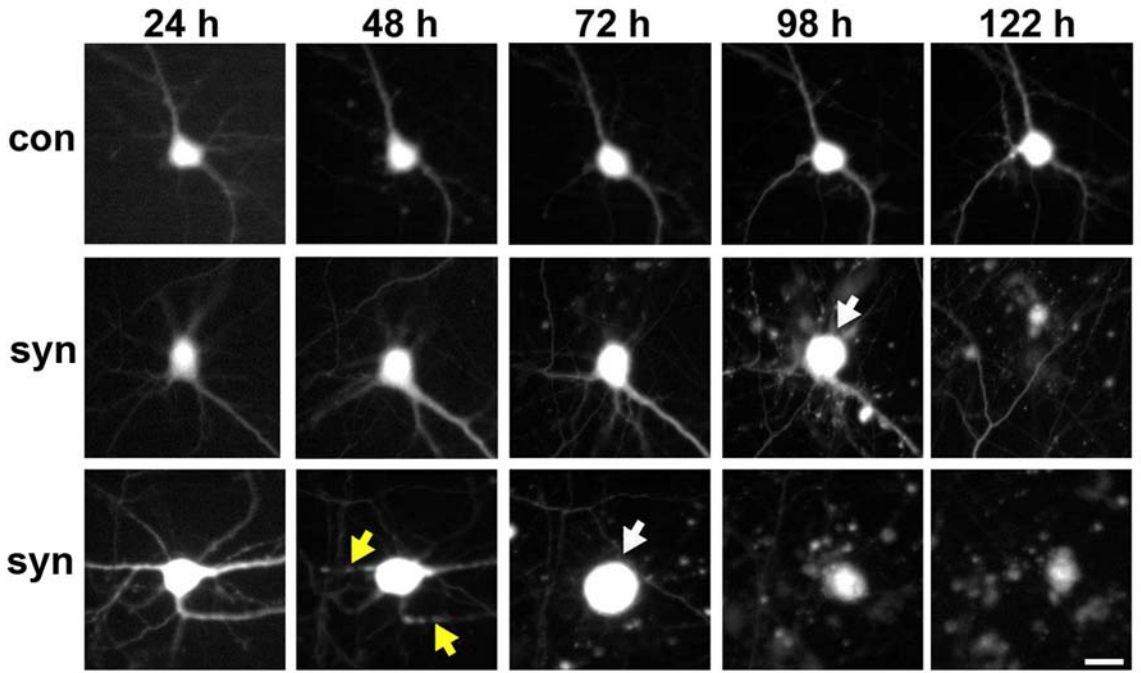

Supplemental Figure 8

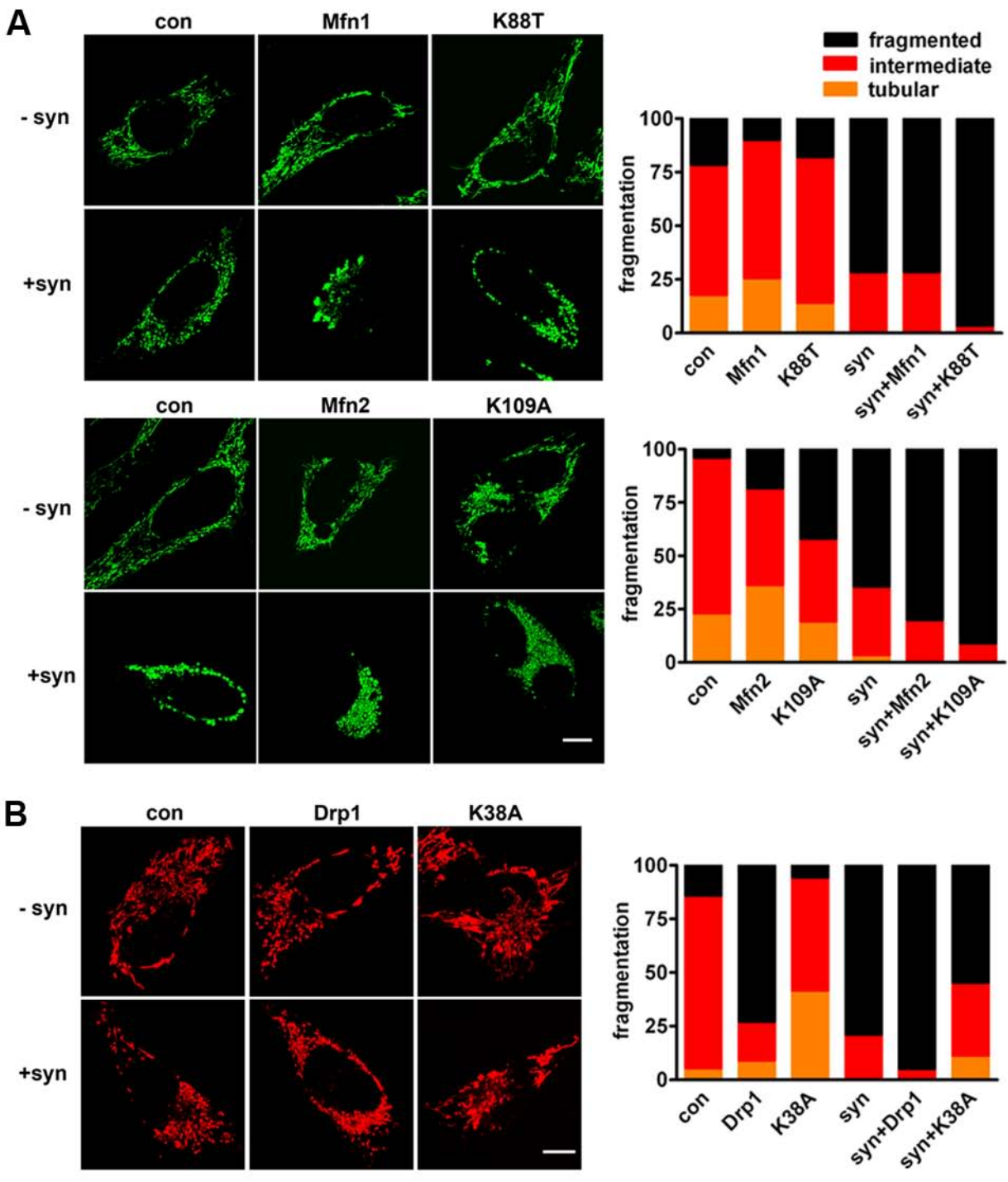

Supplemental Figure 9

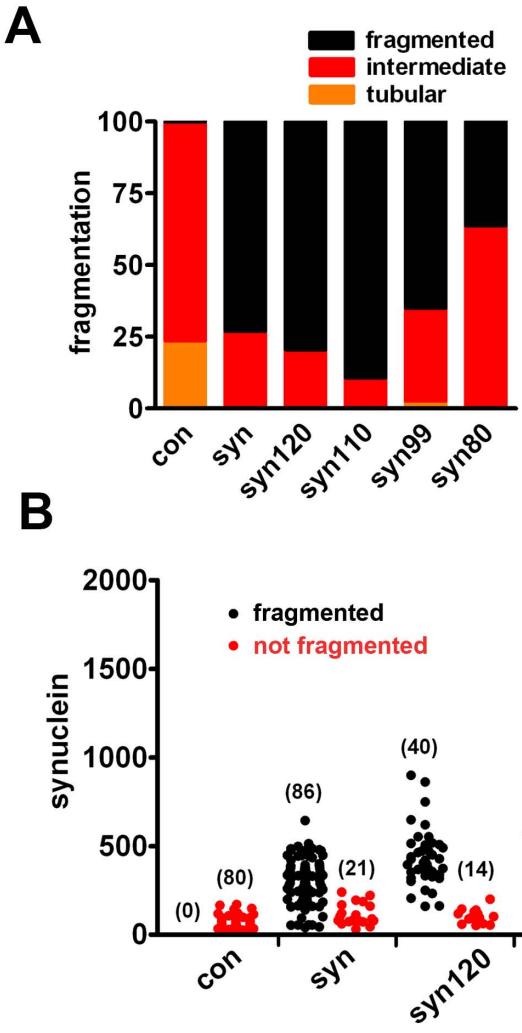

Supplemental Figure 10

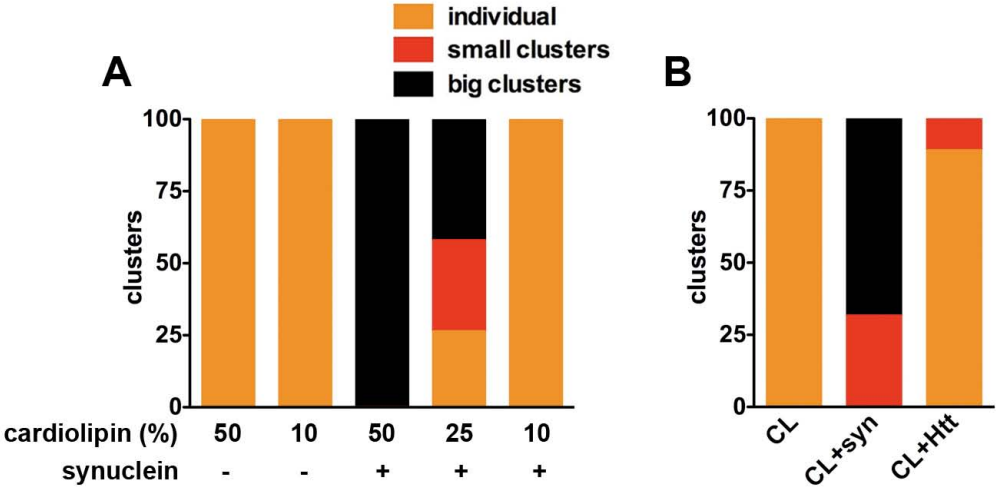

Supplemental Figure 11

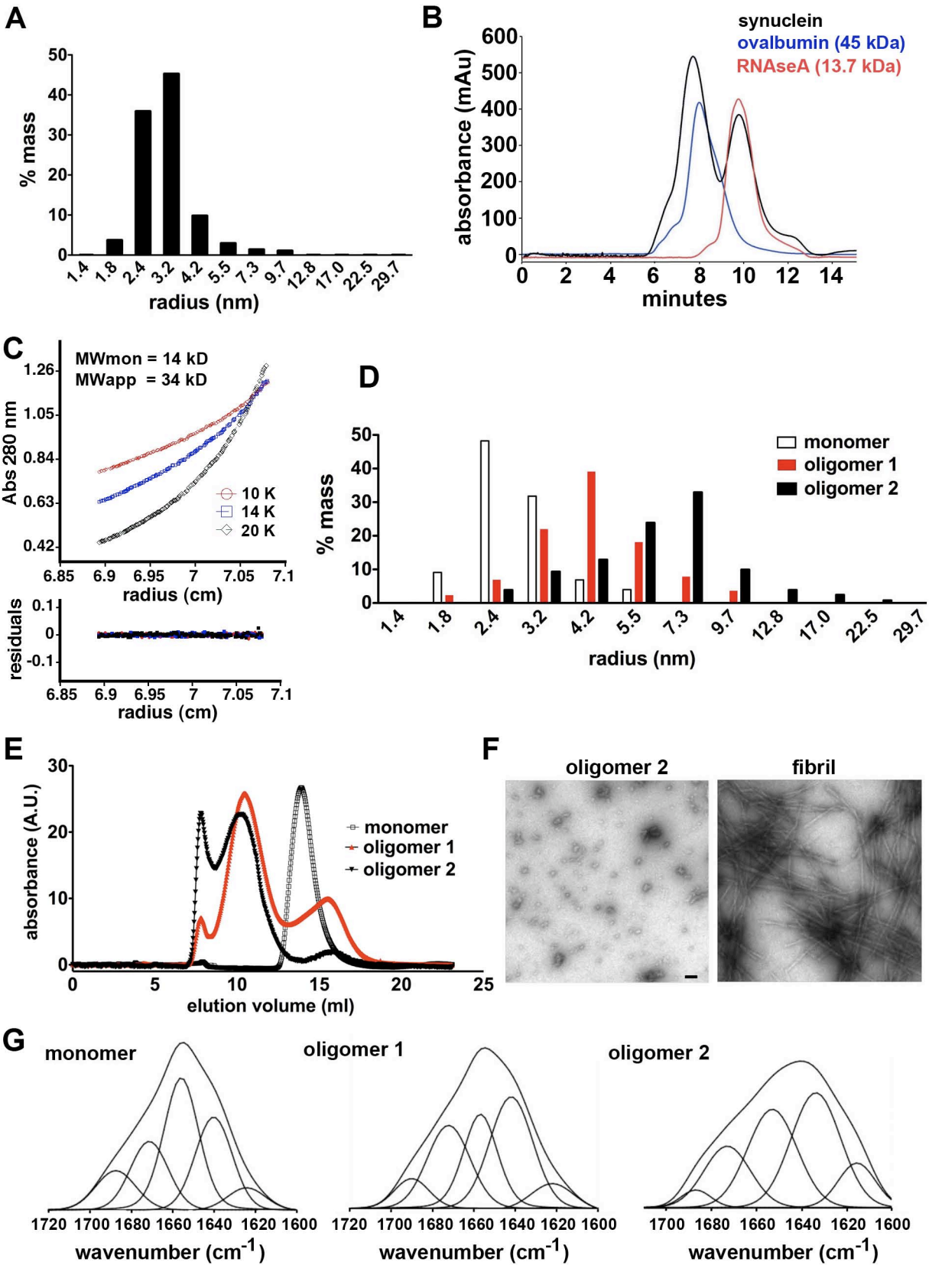

Supplemental Figure 12